DOI: 10.1002/zaac.200801414

$[Cd_3Cu]CuP_{10}$, $[Cd_3Cu]$ Cluster Stabilized in an Adamantane-Like Polyphosphide Substructure

Melanie Bawohl[a] **and Tom Nilges***[a]

Dedicated to Professor Reinhard Nesper on the Occasion of His 60th Birthday

Keywords: Copper; Cadmium; Polyphosphides; Metalloid heteroclusters

Abstract. $[Cd_3Cu]CuP_{10}$ is the first representative of the adamantane-like polyphosphides featuring a metalloid, tetrahedral $[M_3X]$ heterocluster, containing only d^{10} ions. It was prepared by the mineralization concept for polyphosphides using CuI as the mineralizer species. The title compound crystallizes cubic in the space group $F\bar{4}3m$ (No. 216), with a = 10.479(2) Å and V = 1150.9(4) $Å^3$. It is isostructural to the tin containing coinage-metal polyphosphides $[M_3Sn]CuP_{10}$ with M = Cu, Ag, Au. A perfect orientation disorder of the $[Cd_3Cu]$ heterocluster relative to the space diagonals of the cubic cell is present, which is characteristic for the metalloid substructure of this class of compounds. EDX measurements substantiated the refined composition within the standard deviation of the experiment. A slow decomposition of $[Cd_3Cu]CuP_{10}$ was proven by DSC measurements and annealing experiments. The DSC spectra of different samples showed a broad exothermic effect starting at 573 K, which could be identified as a decomposition to new phases. Preliminary results of a single crystal structure determination of the main phase after decomposition pointed towards realized structure units closely related to the title compound, the Cu_2P_{20} and the $[Ag_3Sn]P_7$ structure type. A detailed examination of the structural features of this new compound is still in progress.

Introduction

Polyphosphides containing an adamantane-like polyanion substructure are known for several years now. Beginning with the discovery of $[Cu_3Sn]CuP_{10}$ by *Goryunova* in 1970 [1] and the structure determination later on [2], a recent progress and improvement in the number of new compounds and their chemical understanding was made. By the application of the mineralization concept for polytellurides [3a–c] and polyphosphides [3d–e], capable to prepare compounds featuring 0-dimensional to 2-dimensional polyanionic substructures [4], the synthesis and characterization of $[Ag_3Sn]CuP_{10}$ [5] and $[Au_3Sn]CuP_{10}$ [6] were reported recently. Within the plethora of phosphides and polyphosphides [7] the class of $[P_{10}]$-adamantane containing compounds show some interesting electronic properties, e.g. the metalloid character [8, 9] and the pronounced disorder of the $[M_3Sn]$ groups. Closely related to the $[P_{10}]$-polyphosphides are the $[M_3Sn]P_7$ polyphosphides (M = Ag, Au) [10], which contain a polymeric anion substructure and comparable metalloid clusters.

Reports on tetrahedral building units formed exclusively by late transition metals (d^{10} ions) are rare in the field of carbon-free inorganic chemistry. Pure tetrahedral transition-metal cluster like $[Ag_3Hg]^{3+}$ and $[Ag_2Hg_2]^{4+}$ are known from the mineral tillmansite and closely related compounds [11]. The structure motive of a homoatomic $[Cd_4]$ cluster is known from the intermetallic compounds RE_4TCd (RE = Y, La–Nd, Sm, Gd–Tm, Lu; T = Ni, Pd, Ir, Pt and RE = Y, La–Nd, Sm, and Gd–Tm, Lu; T = Co, Ru and Rh) [12a–b], RE_4CoCd (RE = Tb, Dy, Ho) [12c] and $RE_{23}T_7Cd_4$ [12d]. Cd and mixed Cu/Cd cluster are of various sizes and shapes and are approximants for the structure of Cd_3Cu_4 and i-CdCu [12e–f].

Herein we report on the synthesis and characterization of $[Cd_3Cu]CuP_{10}$, the first compound of an adamantane-type polyphosphide containing a d^{10}-transition-metal heterocluster.

Experimental Section

Synthesis: Cu_3P was prepared from the elements in ideal ratios, prior to use, in evacuated silica ampoules at 823 K. A total amount of 1 g of $[Cd_3Cu]CuP_{10}$ was prepared from a $^2/_3 : 3 : 9^1/_3$ mixture of Cu_3P, cadmium (Chempur, 99.999 %) and phosphorous (Chempur, 99.999+%) in evacuated silica ampoules. The starting materials were heated within 8 h to 1023 K, kept at that temperature for 19 days, and then cooled down to room temperature within 6 h. A second sample (in the following called as cadmium-rich sample), containing starting materials with the ratio Cu_3P/Cd/P = $^2/_3 : 4 : 9^1/_3$ was held at a temperature of 923 K for 14 days before quenching on air. This sample, prepared to identify the decomposition products of $[Cd_3Cu]CuP_{10}$ at elevated temperatures

---

* PD Dr. T. Nilges
E-Mail: nilges@uni-muenster.de
[a] Institut für Anorganische und Analytische Chemie
Westfälische Wilhelms-Universität
Corrensstraße 30
48149 Münster, Germany

(see later on) resulted in a mixture of two phases. The purity of the starting material and the final products was checked by X-ray powder diffraction and EDX analyses.

EDX Measurements: Semi-quantitative analyses were performed with a Leica 420i scanning electron microscope (Zeiss), fitted with an energy dispersive detector unit (Oxford). Cadmium, copper, and GaP (P) were used as standards for calibration. A voltage of 20 kV was applied to the samples. Details concerning the composition of $[Cd_3Cu]CuP_{10}$ are summarized in Table 1.

Table 1. Results from EDX analyses of $[Cd_3Cu]CuP_{10}$, prepared by the mineralization concept using small amounts of CuI. The presence of iodine could not be detected in any measurement.

Sample	Composition (calcd./at-%) Cd/Cu/P	Composition (EDX/at-%) Cd/Cu/P
$[Cd_3Cu]CuP_{10}$ (Crystal 1)	20.0 : 13.3 : 66.7	20(2) : 12(2) : 68(2)
$[Cd_3Cu]CuP_{10}$ (Crystal 2)		21(2) : 14(2) : 65(2)

The results are averaged from 5 to 8 independent measurements for each sample. Standard deviations are estimated from the variations of the measurements. According to Table 1, the averaged value for all analyses results in a composition of $Cd_{3.0(1)}Cu_{1.9(3)}P_{10.0(5)}$, in good accordance with the refined composition derived from single crystal structure determinations.

EDX analyses of selected crystals separated from the bulk residue of the cadmium-rich sample resulted in an averaged composition of Cd/Cu/P = 15 : 2 : 33. Obviously this phase is enriched in Cd compared with the title compound.

X-ray Powder Diffraction: Phase analysis of $[Cd_3Cu]CuP_{10}$ (Figure 1) was performed by X-ray powder diffraction at 293 K. Image plate technology was applied for detection purposes and the read-out was done using a Fuji BAS-1800 reader. Finely ground samples were examined using Guinier cameras, operated with Cu-$K_{\alpha 1}$ radiation (λ = 1.54051 Å, germanium monochromator), and α-quartz was used as an internal standard. All samples were measured at 293 K in transmission geometry.

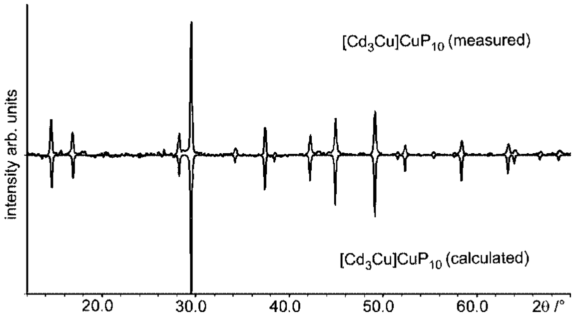

Figure 1. Measured and calculated X-ray powder diffractograms of $[Cd_3Cu]CuP_{10}$. The calculated intensities are drawn downwards for clarity. Space group $F\bar{4}3m$. Lattice parameters derived from powder data are a = 10.479(2) Å, V = 1150.9(5) Å^3 at 293 K.

A rather complex diffractogram was found analysing the cadmium-rich sample prepared at 923 K (see Synthesis section). We could identify at least three different phases of which the minor component was the title compound $[Cd_3Cu]CuP_{10}$.

X-ray Single Crystal Diffraction: Intensity data of two different crystals were collected at 293 K and at 150 K on a STOE IPDS-II image plate system operated with Mo-K_α radiation (λ = 0.71073 Å) in oscillation mode. Temperature-dependent measurements were done using a Cryostream plus system (Oxford). The temperature was calibrated by measuring the two reversible phase transitions of Ag_5Te_2Cl at 244 and 334 K as given in the literature [13]. A tem-

Table 2. Crystallographic data for $[Cd_3Cu]CuP_{10}$, collected from two different crystals at 293 and 150 K (crystal 2 only).

	Crystal 1	Crystal 2	Crystal 2
	(293 K)	(293 K)	(150 K)
Empirical formula		$[Cd_3Cu]CuP_{10}$	
refined composition	$Cd_{2.8(1)}Cu_{2.2(1)}P_{10}$	$Cd_{2.8(1)}Cu_{2.2(1)}P_{10}$	$Cd_{3.2(1)}Cu_{1.8(1)}P_{10}$
Molar mass /g·mol^{-1}	763.3	762.3	782.6
Unit cell dimension a /Å	10.479(2)$^{a)}$	10.479(2)$^{a)}$	10.461(1)
Unit cell volume /Å^3	1150.9(5)	1150.9(5)	1144.8(4)
Z	4	4	4
Calculated density /g·cm^{-3}	4.404	4.398	4.539
Crystal size /mm	0.09 × 0.07 × 0.05	0.10 × 0.07 × 0.05	0.10 × 0.07 × 0.05
Space group		$F\bar{4}3m$	
2θ range	6.74−60.24	6.74−60.0	6.74−60.36
hkl range	−14 to 14 −14 to 14 −14 to 14	−14 to 14 −14 to 14 −14 to 14	−14 to 12 −14 to 14 −14 to 14
Total reflections, R_{int}	3124, 0.0305	3096, 0.0185	2376, 0.0308
No. of parameters	15	15	15
Independent reflections, $R(\sigma)$	214, 0.0125	184, 0.008	205, 0.0161
Flack	0.61(5)	0.55(2)	0.54(3)
Final R indices [$I>3\sigma I$] $R1$	0.0172	0.0110	0.0148
$wR2$	0.0391	0.0181	0.0321
R indices (all data) $R1$	0.0186	0.0116	0.0152
$wR2$	0.0394	0.0181	0.0321
Extinction coefficient	0.045(5)	0.127(4)	0.08(1)
Largest diff. peak and hole /e·Å^{-3}	+0.88/−0.55	+0.93/−0.63	+0.72/−0.52

a) Lattice parameter from X-ray powder diffraction experiment.

Table 3. Coordinates and isotropic displacement parameters for $[Cd_3Cu]CuP_{10}$ at 293 K (crystal 1 and 2) and 150 K (crystal 2).

Atom	sof	x	y	z	U_{iso} /Å^2
Crystal 1 (293 K)					
Cu1	1	0	0	0	0.0076(2)
Cd2	0.70(2)	0.0965(1)	$^1/_2+x$	x	0.0165(1)
Cu2	0.30	0.0965	$^1/_2+x$	x	0.0165
P1	1	0.3715(1)	x	$^1/_2-x$	0.0060(2)
P2	1	$^1/_4$	0.4908(1)	$^1/_4$	0.0103(3)
Crystal 2 (293 K)					
Cu1	1	0	0	0	0.0077(2)
Cd2	0.69(1)	0.0965(1)	$^1/_2+x$	x	0.0161(1)
Cu2	0.31	0.0965	$^1/_2+x$	x	0.0161
P1	1	0.3713(1)	x	$^1/_2-x$	0.0058(2)
P2	1	$^1/_4$	0.4910(1)	$^1/_4$	0.0104(2)
Crystal 2 (150 K)					
Cu1	1	0	0	0	0.0038(1)
Cd2	0.79(2)	0.0964(1)	$^1/_2+x$	x	0.0131(1)
Cu2	0.21	0.0964	$^1/_2+x$	x	0.0131
P1	1	0.3715(1)	x	$^1/_2-x$	0.0034(2)
P2	1	$^1/_4$	0.4909(1)	$^1/_4$	0.0077(2)

Table 4. Selected distances /Å of $[Cd_3Cu]CuP_{10}$ at 293 and 150 K.

$[Cd_3Cu]CuP_{10}$	Cu1−P1	Cd2/Cu2−P2	Cd2/Cu2−Cd2/Cu2	P1−P2
Crystal 1 (293 K)	2.333(1)	2.531(1)	2.859(1)	2.192(1)
Crystal 2 (293 K)	2.336(1)	2.529(1)	2.861(1)	2.192(1)
Crystal 2 (150 K)	2.329(1)	2.526(1)	2.851(1)	2.189(1)

perature deviation of less than 0.1 K from the ideal value was achieved during the measurements.

A correction of Lorentz and polarization effects was applied to the data. The structure was solved by direct methods [14a] from a dataset of crystal 1. We have also performed a numerical absorption correction prior to the refinements [14b], using the measured crystal dimensions determined directly on the diffractometer as starting values for optimization [14c].

One copper, one mixed occupied copper/cadmium and two phosphorus sites were identified after structure solution. All crystallographic data are summarized in Table 2, Table 3 and Table 4.
The heterocluster-position (Cd2/Cu2) showed a significant reduction of the occupancy factor if cadmium alone was selected to occupy this site. A combined refinement of cadmium and copper on this site, only restricted to a full overall occupancy, resulted in a reasonable accordance of the refined to the expected composition.

A reduction of the symmetry to the space group *R*3*m*, resulting in a fourfold twin, with the possibility to achieve an ordered representation of the heterocluster was tested. No evidence for such an ordering could be detected. This finding is in accordance with the results derived from a combined spectroscopic and X-ray scattering approach for $[Ag_3Sn]CuP_{10}$ [5].

Further details of the crystal structure investigations are available from the Fachinformationszentrum Karlsruhe, 76344 Eggenstein-Leopoldshafen (Germany), on quoting the depository number CSD-420224 (293 K, Crystal 1), CSD-420225 (293 K, Crystal 2), and CSD-420226 (150 K, Crystal 2).

Thermal analysis: Thermal analyses (DSC) were performed with a Netzsch DSC 204t instrument in an nitrogen atmosphere in aluminium crucibles. The temperature and enthalpy calibration was done at different temperatures using mercury, indium, tin, bismuth, zinc and CsCl at a heating rate of 10 K/min. An accuracy of ±1 K could be estimated from the calibration measurements for onset values. A temperature range of 173 to 873 K was applied to $[Cd_3Cu]CuP_{10}$ (Figure 2). At least two consecutive runs were measured for each sample in order to check the reversibility of the observed effects.

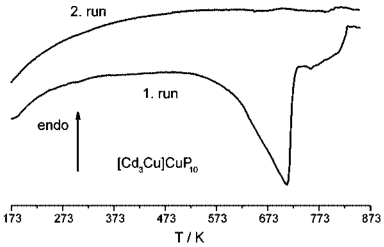

Figure 2. A representative DSC measurement of $[Cd_3Cu]CuP_{10}$ recorded during heating at a scanning rate of 10 K·min^{-1} under nitrogen atmosphere. A broad exothermic effect was found starting at 573 K featuring a peak maximum at 720 K. No such effect was observed in the second run.

We found one broad, irreversible and exothermic effect staring at 573 K with a peak maximum at about 720 K. This effect was reproduceable for independently prepared samples but the start of the effect and the peak maximum varied by several Kelvin from sample to sample. A melting of the compounds was not observed during the measurements up to 873 K, and a X-ray powder phase analysis was performed after the second DSC run.

Results and Discussions

$[Cd_3Cu]CuP_{10}$ crystallizes cubic and isostructural to the $[Cu_3Sn]CuP_{10}$ structure type in space group $F\bar{4}3m$ with a = 10.479(2) Å. Table 5 summarizes some crystallographic data of all known $[P_{10}]$-polyphosphides and gives an overview on the lattice parameter variations dependent on the exchange of the cluster atoms.

$[Cd_3Cu]CuP_{10}$ crystallizes cubic, space group $F\bar{4}3m$ with Z = 4 formula units in the cell. One copper forms a *fcc* cell with half of the tetrahedral voids filled with an adamantane-like $[P_{10}]$ cage and all octahedral voids occupied by a $[Cd_3Cu]$ heterocluster (Figure 3). This heterocluster is characterized by a disorder with a random orientation of one copper atom per cluster in each of the four possible directions.

This finding is consistent with the structural properties of the tin containing heteroclusters reported in the $[M_3Sn]CuP_{10}$ phases. The bond length observed within the $[Cd_3Cu]$ heterocluster is d(Cd2/Cu2−Cd2/Cu2) = 2.859(1) Å. This distance is rather close to the averaged distance of 2.873 Å derived from three times the value for cad-

Table 5. Lattice parameters and effective ionic and atomic radii of all known $[M_3X]CuP_{10}$ compounds. The radii sum (Sum_{CN6}) for all heterocluster atoms in an *anti*-prismatic coordination is calculated. Lattice parameter variations closely related to the volume requirements of the heteroclusters are best described using the atomic instead of the ionic radii.

Compound	a /Å	V /Å^3	Effective ionic radius according to [15]		Atomic radius [16] and radii sum for all $[M_3X]$ atoms		Lit.
$[Cu_3Sn]CuP_{10}$	10.252(1)	1077.6(1)	$Cu^+_{CN\,6}$	0.77	$Cu_{CN\,6}$	1.186	[5]
			$Sn^{2+}_{CN\,6}$	0.93	$Sn_{CN\,6}$	1.530	
			$Sum_{CN\,6}$	3.24	$Sum_{CN\,6}$	5.09	
$[Cu_3Sn]CuP_{10}$	10.267(1)	1082.3(1)					[2]
$[Ag_3Sn]CuP_{10}$	10.503(1)	1158.0(6)	$Ag^+_{CN\,6}$	1.15	$Ag_{CN\,6}$	1.352	[5]
			$Sn^{2+}_{CN\,6}$	0.93	$Sn_{CN\,6}$	1.530	
			$Sum_{CN\,6}$	4.38	$Sum_{CN\,6}$	5.59	
$[Au_{2.41}Cu_{0.59}Sn]CuP_{10}$	10.3953(5)	1123.34(9)	$Au^+_{CN\,6}$	1.37	$Au_{CN\,6}$	1.349	[6]
			$Cu^+_{CN\,6}$	0.77	$Cu_{CN\,6}$	1.186	
			$Sn^{2+}_{CN\,6}$	0.93	$Sn_{CN\,6}$	1.530	
			$Sum_{CN\,6}$	4.69	$Sum_{CN\,6}$	5.48	
$[Cd_3Cu]CuP_{10}$	10.4780(2)	1146.3(3)	$Cd^{2+}_{CN\,6}$	0.95	$Cd_{CN\,6}$	1.453	This work
			$Cu^+_{CN\,6}$	0.77	$Cu_{CN\,6}$	1.186	
			$Sum_{CN\,6}$	3.62	$Sum_{CN\,6}$	5.55	

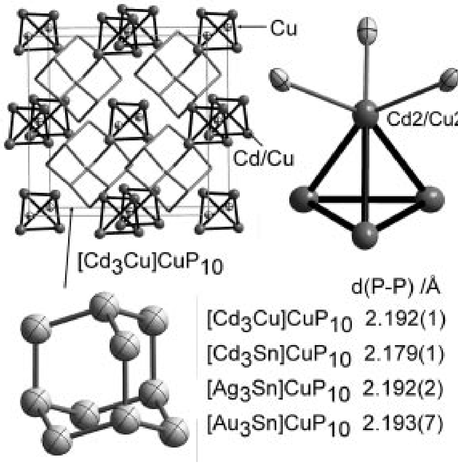

Figure 3. Crystal structure of $[Cd_3Cu]CuP_{10}$. The adamantane-like $[P_{10}]$ cage fills half of the tetrahedral, and the $[Cd_3Cu]$ heterocluster all octahedral voids of a *fcc* arrangement build up by copper. The P−P distances within the $[P_{10}]$ cages are given for comparison. Each Cd2/Cu2 position is antiprismatically coordinated by three cluster and three phosphorus atoms. Displacement parameters at 90 % probability. All literature is cited in the introduction section.

mium d(Cd−Cd) = 2.979 Å [15a] and one time for copper d(Cu−Cu) = 2.556 Å [15b]. It is also located in the bond length range for Cd−Cu bonds of 2.75 to 3.01 Å, as observed for instance in the intermetallic compound Cd_3Cu_4 [12e]. Bond length within the homoatomic $[Cd_4]$ cluster in the intermetallic phases *RET*Cd or $RE_{23}T_7Cd_4$ [12a−d] are slightly longer ranging from 3.00 to 3.25 Å.

Each cluster atom is coordinated *anti*-prismatically to their neighbors and the $[P_{10}]$ cage, featuring a distance of d(Cd2/Cu2−P2) = 2.531(1) Å between the clusters and the $[P_{10}]$ units. In contrast, the bond length d(Cu1−P1) between the isolated cation position and the $[P_{10}]$ unit is 2.3325(9) Å, a well suited value reported for many copper polyphosphides like Cu_2P_7 [d(Cu−P) = 2.27 to 2.40 Å] or CuP_2 [d(Cu−P) = 2.28 to 2.50 Å] [17].

It will be discussed now if the variation of the lattice parameters of $[Cd_3Cu]CuP_{10}$, compared with the other $[M_3Sn]CuP_{10}$ polyphosphides, is a useful probe to reflect the metalloid character of the $[Cd_3Cu]$ unit. Whereas the metalloid character was proven by quantum chemical calculations for $[Ag_3Sn]P_7$ and $[Au_3Sn]P_7$ [8] and by Mössbauer spectroscopy for $[Ag_3Sn]CuP_{10}$ [5], a comparable situation can be estimated for the heteroclusters in all $[M_3X]CuP_{10}$ type compounds. $[Cd_3Cu]CuP_{10}$ crystallizes isostructural to the tin containing compounds. At least the bonding situation and the first coordination sphere, an *anti*-prismatic coordination of each heterocluster atom by three phosphorus atoms of the $[P_{10}]$ units and three cluster atoms, are almost identical in both cases.

Focussing on the title compound and the related polyphosphides it becomes obvious that only the heterocluster unit itself and the interaction with the polyanion substructure can significantly influence the lattice parameters in the present case. The polyanion substructure is rigid and almost unaffected by the exchange of the heterocluster atoms. Bond lengths and angles in the $[P_{10}]$ polyanion differ only marginally and within two times the standard deviation in most of the cases. Because of its comparable bonding situation in each ideal-tetrahedral heterocluster of the $[M_3X]CuP_{10}$ compounds, the radii sum of all atoms is a suitable and sufficient measure for the correlation of the lattice parameter change for all $[M_3X]CuP_{10}$ compounds. The radii sum used here is defined as the sum of all ionic or atomic radii of the heterocluster atoms corrected to their coordination sphere. We have applied an ionic and metallic approach to the heterocluster atoms in terms of the description of the respective radii.

Taking the ionic representation of the cluster atoms into account, as stated for the respective ions in a six fold coordination in Table 5, the lattice parameter of $[Cd_3Cu]CuP_{10}$ should be closely related to $[Cu_3Sn]CuP_{10}$. In contrast, the observed value lies closer to the one found for

$[Ag_3Sn]CuP_{10}$. Only the atomic radii, derived from the distance in the respective elements, and corrected to the coordination number 6, according to the procedure stated in literature ($r_{CN\,6} = r_{CN\,12}-0.090$) [16], lead to a straight forward and linear correlation of lattice parameter and the radii sum of atoms of the heterocluster.

In the case of the atomic radii its values are corrected to the radii within the respective coordination sphere (here it is CN = 6). Figure 4 illustrates the radii sum for all heteroclusters in correlation with the lattice parameter of the respective compound. A linear trend can be observed, substantiating the metalloid character of the heteroclusters. Following the Zintl concept a formal charge of +7 ($3 \times Cd^{2+}$ and Cu^{+}) would result for the heterocluster and +1 for the additional copper cation which can not be compensated by the $[P_{10}]$ unit only containing six two-bonded P positions of formal charge −1. The charge of the heterocluster must be significantly reduced to derive a reasonable description of the electronic situation in the title compound.

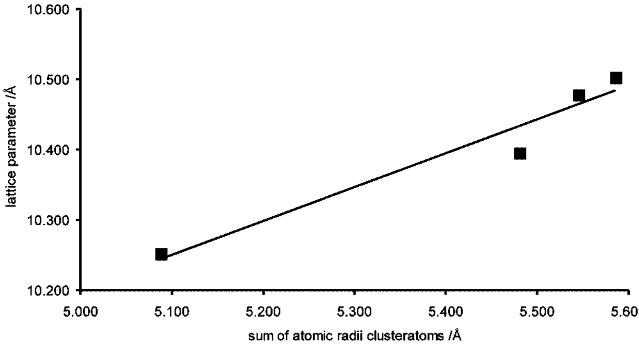

Figure 4. Correlation between the sum of the atomic radii of the cluster atoms in relation to the lattice constant of the isostructural $[M_3X]CuP_{10}$ compounds.

The open question whether an orientation or substitution disorder is present in the heterocluster of $[Cd_3Cu]CuP_{10}$ can not be answered completely at this point. Copper and cadmium sometimes show the tendency to occupy the same sites in intermetallic compounds as shown for instance in Cd_3Cu_4 [12e] or the γ-brass compound $Cd_{7.75}\,Cu_{5.25}$ [18]. Also a huge number of ordered binary and ternary intermetallics (e.g. Cd_5Cu_2 [19] or $RECu_4Cd$ [20]) are reported in the literature. Taking the structural features of the tin containing polyphosphides into account a substitution disorder, resulting in the realization of $[Cd_4]$ and $[Cd_2Cu_2]$ cluster, is at least less probable. Additional experiments using local probes like solid state NMR spectroscopy is needed in the future to finally answer this question.

$[Cd_3Cu]CuP_{10}$ is characterized by a surprising reactivity upon heating. We found an irreversible, broad and exothermic effect in the DSC experiment which was never observed before for any of the known $[P_{10}]$ polyphosphides. A X-ray powder diffraction phase analysis after two consecutive DSC runs is given in Figure 5. We found additional reflections beside the ones of $[Cd_3Cu]CuP_{10}$ in the diffractogram which could not be correlated to any known cadmium, copper, phosphorus or iodine containing phase. Obviously, the crystallinity of the decomposition products is low, resulting only in small contributions to the diffractogram. In order to put some light onto this feature we have tried to identify the products to get more information related to this aspect. If the composition is slightly varied towards a cadmium-rich one and the synthesis conditions are modified in terms of the applied reaction temperatures (annealing at 923 K

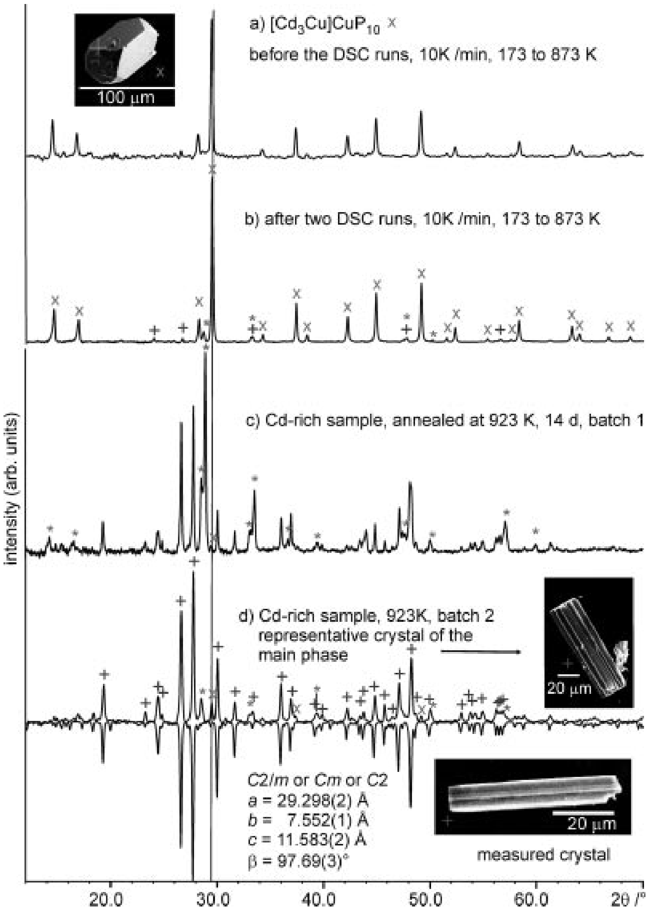

Figure 5. Phase analyses of $[Cd_3Cu]CuP_{10}$ before and after the DSC measurement and results of the cadmium-rich sample. a) Diffractogram of $[Cd_3Cu]CuP_{10}$ (reflections are marked x) prior to the DSC measurements. A representative crystal of $[Cd_3Cu]CuP_{10}$ is printed into the top diffractogram b). A slow decomposition was observed by DSC, resulting in additional reflections in the diffractogram (+). These reflections are identical to the strongest reflections observed in the cadmium-rich sample which was annealed at 923 K for 14 days denoted in c) and d). $[Cd_3Cu]CuP_{10}$ is only the minority phase in this cadmium-rich sample. d) A calculated diffractogram derived from a preliminary structure determination of the main phase (+) using the space group *C2/m* is given. One representative crystal of this phase and also the measured crystal are given in the last diffractogram. A vertical line is provided to guide the eyes and to illustrate the strongest reflection of $[Cd_3Cu]CuP_{10}$. A third unknown phase (*) is also present in c) and d).

and quenching instead of 1023 K and a slow cool-down to room temperature), the title compound has not been found in reasonable amounts any more. A complex mixture of at least three different phases was found instead (see Figure 5) where the title compound is only the minority compound. Both additional phases are possible candidates to be formed after the decomposition of $[Cd_3Cu]CuP_{10}$ which can be estimated from the occurrence of the strongest reflections in the diffractogram after the DSC experiment. Additional experiments have to be done to explain the fact that no thermal effect is observed in the second DSC run while the majority of $[Cd_3Cu]CuP_{10}$ seemed not to be decomposed [see b) in Figure 5] after the experiment.

Preliminary results of single crystal structure determinations of one of the resulting phases substantiated the occurrence of some structural features of the $[Ag_3Sn]P_7$ [3a] and the Cu_2P_{20} structure type [3b]. It was possible to reduce the space groups to *C*2/*m*, *Cm* or *C*2 for this phase. A calculated powder diffractogram using the space group *C*2/*m* was used to identify the main phase. A full structure determination is still in progress and will be reported soon. Then we will be able to give a full description of the phase relations in the present case.

The slightly different starting composition, the morphology of $[Cd_3Cu]CuP_{10}$ compared with the new cadmium-rich phase and also the pronounced texture of the crystals (see Figure 5) may lead to the assumption that the new phase is formed after the decomposition of $[Cd_3Cu]CuP_{10}$ of the phase pure sample during the DSC experiment. Recently, it was shown, for instance with the rapid preparation of black phosphorus [4d], $Pb_5I_2P_{28}$ [4b] or $AgSbP_{14}$ [4a] that the mineralization concept is capable to promote complex gas phase reactions leading to unexpected and rather complex polyphosphides at low reaction times. Black phosphorus can be grown in a DSC ampoule during a measurement at $10\ K\cdot min^{-1}$ between room temperature and 923 K using the mineralization concept [21]. It will be a challenging project in the future, which is not only related to this special case, to examine the present gas phase species and to illuminate the basic formation principles of compounds prepared by the mineralization concept.

Conclusions

The discovery of $[Cd_3Cu]CuP_{10}$ extends the chemistry of tetrahedral metalloid heteroclusters in $[P_{10}]$ polyphosphide chemistry to homonuclear d^{10} transition elements. It clearly reflects the fact that a Zintl-like description is not an adequate model to describe the structural properties of this new compound. Single crystal structure determinations at various temperatures did not result in any hints for an ordering of the $[Cd_3Cu]$ heteroclusters. The orientation disorder of this group remained down to a temperature of 150 K. This finding is in good accordance to the results reported for the $[M_3Sn]CuP_{10}$ polyphosphides. $[Cd_3Cu]CuP_{10}$ decomposes slowly at temperatures above 573 K to new phases of which at least one contains more cadmium than the title compound itself. A first structural characterization of the majority phase, which we have found after a preparation using more cadmium compared to the ideal composition in $[Cd_3Cu]CuP_{10}$, substantiated the occurrence of known structure motives found in polyphosphides like Cu_2P_{20} and $[M_3Sn]P_7$ (M = Ag, Au).

Acknowledgement

This work was financed by the *DFG* with the grant *NI 1095/1−1*.

References

[1] N. A. Goryunova, V. M. Orlov, V. I. Sokolova, G. P. Shepenkov, E. V. Tsvetkova, *Phys. Status Solidi A* **1970**, *3*, 75.

[2] W. Hönle, H. G. von Schnering, *Z. Kristallogr.* **1980**, *153*, 339.

[3] a) T. Nilges, S. Lange, M. Bawohl, J. M. Deckwart, M. Janssen, H.-D. Wiemhöfer, R. Decourt, B. Chevalier, J. Vannahme, H. Eckert, R. Weihrich, *Nature Mater.* **2009**, *8*, 101; b) S. Lange, M. Bawohl, D. Wilmer, H.-W. Meyer, H.-D. Wiemhöfer, T. Nilges, *Chem. Mater.* **2007**, *19*, 1401; c) S. Lange, T. Nilges, *Chem. Mater.* **2006**, *18*, 2538; d) M. M. Shatruk, K. A. Kovnir, A. V. Shevelkov, B. A. Popovkin, *Angew. Chem.* **2000**, *112*, 2561; *Angew. Chem. Int. Ed.* **2000**, *39*, 2508; e) S. Lange, M. Bawohl, R. Weihrich, T. Nilges, *Angew. Chem.* **2008**, *120*, 5736; *Angew. Chem. Int. Ed.* **2008**, *47*, 5654.

[4] a) S. Lange, C. P. Sebastian, T. Nilges, *Z. Anorg. Allg. Chem.* **2006**, *632*, 195; b) M. Bawohl, T. Nilges, *Z. Anorg. Allg. Chem.* **2009**, DOI: 10.1002/zaac.200801285; c) S. Lange, P. Schmidt, T. Nilges, *Inorg. Chem.* **2007**, *46*, 4028; d) T. Nilges, M. Kersting, T. Pfeifer, *J. Solid State Chem.* **2008**, *181*, 1707.

[5] S. Lange, C. P. Sebastian, L. Zhang, H. Eckert, T. Nilges, *Inorg. Chem.* **2006**, *45*, 5878.

[6] S. Lange, T. Nilges, *Z. Naturforsch.* **2006**, *61b*, 871.

[7] a) R. Pöttgen, W. Hönle, H. G. von Schnering in *Encyclopedia of Inorganic Chemistry*, Vol. VIII, 2nd ed. (Ed.: R. B. King), Wiley, Chichester, 2005; b) H. G. von Schnering, *Chem. Rev.* **1988**, *88*, 243−273.

[8] R. Weihrich, S. Lange, T. Nilges, *Solid State Sci.* **2008**, DOI: 10.1016/j.solidstatesciences.2008.09.005, in press.

[9] D. W. Bullet, W. G. Dawson, *Solid State Commun.* **1986**, *60*, 767.

[10] S. Lange, P. Schmidt, T. Nilges, *Inorg. Chem.* **2006**, *46*, 4028.

[11] a) H. Sarp, D. Y. Pushcharovsky, E. J. MacLean, S. J. Teat, N. V. Zubkova, *Eur. J. Mineral.* **2003**, *15*, 177; b) M. Weil, E. Tillmanns, D. Y. Pushcharovsky, *Inorg. Chem.* **2005**, *44*, 1443.

[12] a) F. M. Schappacher, U. Ch. Rodewald, R. Pöttgen, *Z. Naturforsch.* **2008**, *63b*, 1127; b) F. M. Schappacher, R. Pöttgen, *Monatsh. Chem.* **2008**, *139*, 1137; c) A. Doğan, S. Rayaprol, R. Pöttgen, *J. Phys.: Condens. Matter* **2007**, *19*, 076213; d) F. Tappe, R. Pöttgen, *Z. Naturforsch.* **2009**, *64b*, in press; e) S. Samson, *Acta Crystallogr.* **1967**, *23*, 586; f) G. Kreiner, M. Schäpers, *J. Alloys Compd.* **1997**, *259*, 83.

[13] T. Nilges, S. Nilges, A. Pfitzner, T. Doert, P. Böttcher, *Chem. Mater.* **2004**, *16*, 806.

[14] a) G. M. Sheldrick, *SHELX-97*, Program for Crystal Structure Solution and Refinement, University of Göttingen, Göttingen (Germany) **1997**; b) V. Petříček, M. Dušek, L. Palatinus, *JANA2000*, The Crystallographic Computing System, Institute of Physics, Praha (Czech Republic) 2000; c) *X-RED 32*, version 1.10 and *X-SHAPE*, version 2.05; Stoe & Cie GmbH Darmstadt, Germany, **2004**; d) *WinXpow*, version 1.25; Stoe & Cie GmbH Darmstadt, Germany, **2004**.

[15] a) R. D. Shannon, C. T. Prewitt, *Acta Crystallogr., Sect. B* **1969**, *25*, 925; b) R. D. Shannon, *Acta Crystallogr., Sect. A* **1976**, *32*, 751.

[16] L. Pauling, *J. Am. Chem. Soc.* **1947**, *69*, 542.
[17] M. Möller, W. Jeitschko, *Z. Anorg. Allg. Chem.* **1982**, *491*, 225.
[18] J. K. Brandon, R. Y. Brizard, P. C. Chieh, R. K. McMillan, W. B. Pearson, *Acta Crystallogr., Sect. B* **1974**, *30*, 1412.
[19] T. Rajasekharan, K. Schubert, *Z. Metallk.* **1982**, *73*, 262.
[20] R. Pöttgen, A. Doğan, *Z. Naturforsch.* **2005**, *60b*, 495.
[21] S. Lange, M. Bawohl, T. Nilges, unpublished results.

Received: December 23, 2008